Journal of Biotechnology 143 (2009) 213–223

Contents lists available at ScienceDirect

Journal of Biotechnology

journal homepage: www.elsevier.com/locate/jbiotec

Effect of CO_2 on succinate production in dual-phase *Escherichia coli* fermentations

Shiying Lu, Mark A. Eiteman*, Elliot Altman

Center for Molecular BioEngineering, University of Georgia, Athens, GA 30602, United States

ARTICLE INFO

Article history:
Received 6 March 2009
Received in revised form 14 June 2009
Accepted 12 July 2009

Keywords:
PEP carboxylase
^{13}C-labeling
Metabolic flux analysis
Succinic acid

ABSTRACT

Succinate production under different concentrations of carbon dioxide (CO_2) was studied in *Escherichia coli* AFP111, which contains mutations in pyruvate formate lyase (*pfl*), lactate dehydrogenase (*ldhA*) and the phosphotransferase system glucosephosphotransferase enzyme II (*ptsG*). A series of two-phase fermentations were conducted in which an aerobic cell growth phase was followed by an anaerobic succinate production phase using several constant concentrations of CO_2. As the concentration of CO_2 in the gas phase increased from 0% to 50%, the succinate specific productivity increased from 1.9 mg/g h to 225 mg/g h, and the succinate yield increased from 0.04 g/g to 0.75 g/g. Above 50% CO_2, succinate production did not increase further. Intracellular fluxes were determined at three different CO_2 concentrations (3%, 10%, and 50%) using ^{13}C-label tracing coupled with LC–MS analysis. The fraction of carbon flux into the pentose phosphate pathway increased from 0.04 at 3% CO_2 to 0.17 at 50% CO_2. Also, the fractional flux through anaplerotic carboxylation at the phosphoenolpyruvate (PEP) node increased slightly from 0.53 at 3% CO_2 to 0.63 at 50% CO_2. The increased flux into the pentose phosphate pathway is attributed to an increased demand for reduced cofactors with elevated CO_2. A four-process explicit model to describe the CO_2 transfer and utilization was proposed. The model predicted that at CO_2 concentrations below about 30–40% the system becomes limited by gas phase CO_2, while at higher CO_2 concentrations the system is limited by PEP carboxylase enzyme kinetics.

1. Introduction

Microbial "sequestration" of carbon dioxide (CO_2) has centered on *bacteria* and *archaea* (Shively et al., 1998; Atom, 2002) in liquid suspension or microalgal systems (Brown, 1996; Watanabe and Hall, 1996). Photosynthesis is often required for CO_2 fixation, which limits the application of biological CO_2 sequestration due to scale-up problems (Zhang et al., 2002). In addition, many microorganisms considered for CO_2 fixation have fastidious growth requirements, and have unacceptably low product yields and formation rates (Shively et al., 1998; Atom, 2002). For example, Otsuki (2001) reported a CO_2 volumetric utilization rate of only 13 mg CO_2/L h. Substrate consumption and product formation rates are generally more than 100-fold greater in commercially relevant microbial based systems.

Another goal for CO_2 sequestration processes is that a "product" be generated. A saleable product from CO_2 would defray costs associated with CO_2 sequestration. For algal processes, examples include β-carotene, pigments, animal feed and cosmetics (Fleurence, 1999; Spolaore et al., 2006). For biological sequestration of CO_2, ultimately an enzyme must incorporate CO_2 into the backbone of one organic compound (C_X) to generate another larger organic compound (C_{X+1}). Therefore, another approach for generating a product microbially using CO_2 would involve transforming an inexpensive C_X compound to a more valuable C_{X+1} compound. Potential examples of this strategy include the enzymes phosphoenolpyruvate (PEP) carboxylase (PPC, EC 4.1.1.31), PEP carboxykinase (PCK, EC 4.1.1.49) and pyruvate carboxylase (PYC, EC 6.4.1.1), each of which converts PEP or pyruvate (C_3) into oxaloacetate (C_4). In practice, these enzymes might convert a substrate upstream of CO_2 fixation (such as glycerol or glucose) into a product downstream of a CO_2 fixation step (such as succinic acid).

As a model system, *Escherichia coli* can sequester CO_2 through native PPC (Matsumura et al., 2002), PCK (Matte et al., 1997), or heterologous PYC (Modak and Kelly, 1995) to generate succinate. Although aerobic growth generates CO_2, a biocatalytic process would consume CO_2 under non-growing anaerobic conditions. *E. coli* with mutations in the lactate dehydrogenase (*ldhA*), pyruvate formate lyase (*pfl*) and phosphotransferase system glucosephosphotransferase enzyme II (*ptsG*) genes that also expresses heterologous PYC generates about 100 g/L succinate with an overall productivity of 1.3 g/L h and based on stoichiometric considerations should consume CO_2 at a volumetric rate of about 240 mg/L h (Vemuri et al., 2002a,b), an order of magnitude faster than comparable phototrophic processes that have been studied.

Succinate is formed through two pathways: one is the reductive arm of the tricarboxylic acid cycle (TCA) through the anaplerotic

* Corresponding author. Tel.: +1 706 542 0833; fax: +1 706 542 8806.
E-mail address: eiteman@engr.uga.edu (M.A. Eiteman).

0168-1656/$ – see front matter © 2009 Elsevier B.V. All rights reserved.
doi:10.1016/j.jbiotec.2009.07.012

enzyme PPC, and the other is the glyoxylate shunt (Vemuri et al., 2002b). The former incorporates CO_2 into central metabolism, and one objective of this study was to elucidate the cellular requirement for CO_2. Also, different CO_2 concentrations may change the fractions of succinate that partitions between these and other key pathways. In this study, metabolic flux analysis coupled with ^{13}C-labeling tracing was employed to determine the metabolic fluxes at various CO_2 concentrations. The overall goal is to understand how the CO_2 concentration in the gas phase affects metabolic fluxes during the succinate production phase and to clarify what aspect(s) of the process may be limiting under various CO_2 concentrations. Glucose labeled at the C-1 position was used because this isotopomer is excellent for determination of the metabolic partitioning of glucose (Ugurbil et al., 1978; McKinlay et al., 2007), and because as the product succinate is symmetric, a label at this position was found by isotopomer analysis to generate the most distinguishing succinate isotopomer patterns.

2. Materials and methods

2.1. Strain

E. coli AFP111 (F^+ λ^- *rpoS*396 (Am) *rph*-1 Δ*pflAB*::Cam *ldhA*::Kan *ptsG*) was used in this study, which has mutations in the fermentative genes encoding for pyruvate formate lyase and lactate dehydrogenase, and has a disruption in the phosphotransferase system for glucose uptake (Donnelly et al., 1998; Chatterjee et al., 2001).

2.2. Fermentation media

All fermentations used a defined medium containing (per L): 40.0 g glucose, 3.0 g citric acid, 3.0 g $Na_2HPO_4{\cdot}7H_2O$, 8.00 g KH_2PO_4, 8.00 g $(NH_4)_2HPO_4$, 0.20 g NH_4Cl, 0.75 g $(NH_4)_2SO_4$, 1.00 g $MgSO_4{\cdot}7H_2O$, 10.0 mg $CaCl_2{\cdot}2H_2O$, 0.5 mg $ZnSO_4{\cdot}7H_2O$, 0.25 mg $CuCl_2{\cdot}2H_2O$, 2.5 mg $MnSO_4{\cdot}H_2O$, 1.75 mg $CoCl_2{\cdot}6H_2O$, 0.12 mg H_3BO_3, 1.77 mg $Al_2(SO_4)_3{\cdot}xH_2O$, 0.5 mg $Na_2MoO_4{\cdot}2H_2O$, 16.1 mg Fe(III) citrate, 20 mg thiamine·HCl, and 2 mg biotin.

2.3. Fermentation conditions

Dual-phase fermentations had an initial volume of 1.2 L in 2.5-L fermenters (Bioflwo III, New Brunswick Scientific, Edison, NJ, USA) inoculated from 50 mL grown for 10–12 h in the same medium in 250 mL shake flasks. Oxygen-enriched air as necessary was sparged at 1.0 L/min with an agitation of 200–500 rpm to maintain the dissolved oxygen (DO) above 40% (Mettler-Toledo Process Analytical Instruments, Wilmington, MA, USA). During growth, the pH was controlled at 7.0 with 20% NaOH and 20% H_2SO_4, and the temperature was maintained at 37 °C. When the culture optical density (OD_{600}) reached about 20, the aerobic growth phase was terminated by switching the inlet gas composition to the particular mixture under study. Simultaneously, the total flowrate was reduced to 500 mL/min (dry basis, 0 °C and 1 atm), the pH was controlled at 6.4, the agitation reduced to 200 rpm, 20% NaOH was replaced by 25% $Ca(OH)_2$ as the neutralizing agent, and 120 mL of a 550 g/L glucose solution was added to increase the concentration to about 60 g/L. Because calcium salts generate some precipitate, OD was not determined during the anaerobic phase. In previous research, we have observed only a slow decline in viable cell count during the first 10–15 h of anaerobic conditions (unpublished).

The effect of CO_2 on succinate production at a pH of 6.4 was examined by controlling the proportion of CO_2 and N_2 flowrates in the influent gas using mass flow controllers (Unit Instruments, Inc., Yorba Linda, CA, USA) Gases were pre-humidified in 300 mm × 50 mm glass columns (Ace Glass Inc., Vineland, NJ, USA) before entering the fermenter. Fig. 1 shows the setup for the anaerobic production phase.

For studies involving [1-^{13}C] glucose, dual-phase fermentations were repeated as described above except the initial volume was 0.6 L in 1.0-L fermenters (Bioflow III, New Brunswick Scientific, Edison, NJ, USA), the inoculum volume was reduced to 25 mL and the

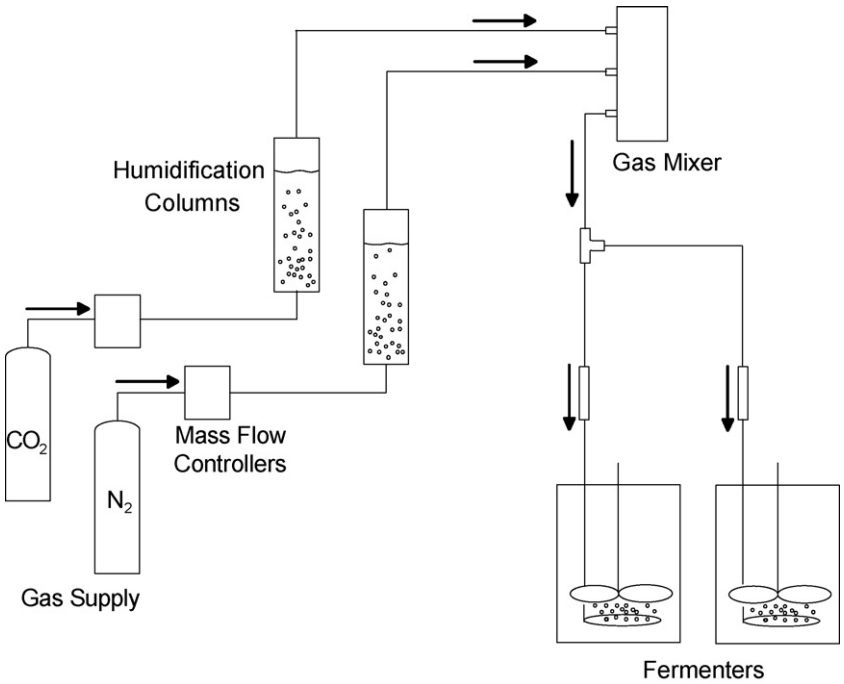

Fig. 1. Setup of gas supply system for study of anaerobic production of succinate using *E. coli* AFP111. Nitrogen and carbon dioxide were proportioned into each 1.2 L culture volume at a total flowrate of 500 mL/min (dry basis, 1 atm, 0 °C).

initial glucose concentration was 30 g/L. The glucose concentration was monitored using a glucose analyzer (YSI 2700 SELECT™, Yellow Springs Instrument, Inc., Yellow Springs, OH, USA). When the glucose concentration reached 2 g/L, the system was switched to anaerobic conditions by sparging the desired CO_2 and N_2 gas mixture. When the glucose concentration reached 1 g/L, 2.5 g [1-^{13}C] glucose (99%, Cambridge Isotope Laboratories, Andover, MA, USA) was added into the fermenter. Samples were then collected every 30 min, centrifuged at 0 °C (10,000 × *g* for 10 min), and the supernatants stored at −4 °C for later NMR and LC–MS analysis.

2.4. LC–MS analysis of succinate

The sample supernatant was filtered by 0.2 μM syringe filter (Cole-Parmer Instrument Co., Vernon Hills, IL, USA) prior to LC–MS analysis. The liquid chromatography was performed (Applied Biosystems 140B Solvent Delivery System, Applied Biosystems, Foster City, CA, USA) using C18 column (Kromasil, 250 mm × 1 mm, 5 μm particles, 100 Å pore space, Keystone Scientific, Inc., Bellefonte, PA, USA). The mobile phase was a gradient consisting of aqueous acetic acid (0.1%, w/v, pH 3.23) and methanol. The mobile phase flowrate was 50 μL/min, and the temperature was 25 °C. Electrospray ionization mass spectrometry was performed using a single quadrupole instrument with electrospray ion source (API 1 Plus, PE Sciex, Concord, ON, Canada), operating with nebulizer gas (N_2) at a flowrate of 0.6 L/min and pressure of 30 psi, curtain gas (N_2) at a flowrate of 0.8 L/min, and interface temperature of 50 °C. Data were acquired in negative ion mode with a capillary voltage of 3500 V. Mass peak heights were determined using the BioTool Box Version B software package (Applied Biosystems/PE Sciex, Foster City, CA, USA). The relative concentrations of M + 0, M + 1, M + 2, and M + 3 (M + 0 represents succinate without ^{13}C-label having a m/z of 117, etc.) were calculated by the fractions of each peak heights after correcting for naturally occurring ^{13}C (1.109%) and ^{18}O (0.20%) (Rosman and Taylor, 1998).

2.5. Metabolic modeling and flux analysis

An overall flux balance was developed using stoichiometric analysis and the pseudo-steady-state condition for intracellular metabolites (Savinell and Palsson, 1992). The balance equations for *E. coli* AFP111 metabolism have been developed previously (Vemuri et al., 2002a), and this model was further extended by including the pentose phosphate pathway (Fig. 2). Flux partitions (φ) were defined as fractional fluxes (ν) for each of two key branches. The fraction of flux into the pentose phosphate pathway (φ_{PPP}) was defined as

$$\varphi_{PPP} = \frac{\nu_3}{\nu_2 + \nu_3}$$

The fraction of flux through anaplerotic carboxylation at the PEP node (φ_{PPC}) was defined as:

$$\varphi_{PPC} \frac{\nu_{13}}{\nu_{13} + \nu_{14}}$$

The model contained 27 fluxes and 21 metabolites (Fig. 2 and Appendix A). Since no growth occurred during the anaerobic process (Vemuri et al., 2002b), glucose consumption and product formation rates were essentially constant; thus the process exhibited a metabolic pseudo-steady-state. Although five fluxes were known, the balance equations represent an underdetermined set. The MS results using 1-^{13}C-glucose allowed us to calculate the error-minimized solution. Specifically, we wrote analogous balance equations for each isotopomer of each metabolite (Schmidt et al., 1997). We calculated the distribution of succinate isotopomers for a given set of fluxes and calculated the mole fraction (X_{calc}) of each isotopomer i. These calculated values were compared with the mole fractions of each isotopomer observed from the LC–MS results (X_{obs}). The solution for the flux model was then determined by minimizing the weighted sum of squared residuals over the four mass peaks (Van Dien et al., 2003):

$$\text{error} = \sqrt{\sum_{i=0}^{3} \frac{(X_{calc,i} - X_{obs,i})^2}{s_i^2}}$$

where s is the standard deviation of the observed mole fraction, determined by three LC–MS analyses of each sample. The isotopomer analysis cannot determine whether the malic enzyme and pyruvate oxidase were active because the ^{13}C-labeled patterns resulting from these pathways are indistinguishable from the PPC and pyruvate dehydrogenase–phosphotransacetylase–acetate kinase pathways, respectively. Therefore, the model did not include these two pathways.

2.6. NMR analysis of succinate

The sample supernatant was filtered by 0.2 μM syringe filter (Cole-Parmer Instrument Co., Vernon Hills, IL, USA), and then the filtered supernatant was mixed with 15% volume of deuterium dioxide (D_2O) for nuclear magnetic resonance (NMR) analysis. Proton-coupled ^{13}C NMR spectra at 125.7 MHz were obtained with the following spectral parameters: 45° pulses, 31.4-kHz spectral width, and 45 s relaxation delay (Varian Unity Inova 500; Varian Inc., Palo Alto, CA. USA). Field stabilization was achieved by locking on the D_2O frequency. ^{13}C chemical shift assignments for succinate were determined by comparison with a natural abundance standard.

NMR was not used to calculate fluxes, but was employed to complement the LC–MS results with an independent measurement. Specifically, since the mass spectra did not provide information about the position of the label, we used NMR to observe the total ^{13}C enrichment at C-1 position (S1) and that at C-2 position of succinate (S2). The enrichment ratio of S2/S1 was calculated from the ratio of peak area of methylene group to carboxyl group of succinate. This observed enrichment ratio was compared to the enrichment ratio calculated from the error-minimized metabolic flux model. Furthermore, anaerobic pathways involved in succinate formation require cofactors NAD(P) and NAD(P)H. The rates of formation of the oxidized and reduced forms must balance. To further validate the error-minimized model, therefore, we calculated the R/O ratio as the sum of the NAD(P)H generating fluxes through the metabolic pathways to the sum of the NAD(P)H-consuming fluxes.

2.7. HPLC analysis of glucose and products

Samples were diluted by 1% H_2SO_4 as necessary, centrifuged (10,000 × *g* for 10 min at 4 °C), and the supernatant analyzed for glucose and organic products by high performance liquid chromatography (HPLC) as previously described (Eiteman and Chastain, 1997).

2.8. Enzyme assays

Cell extracts of the *E. coli* strains were prepared by washing the cell pellets with an appropriate buffer and disrupting the suspended cells with an SLM-Aminco French pressure cell (Spectronic Instruments, Rochester, NY, USA) at a pressure of 14,000 lb/in.^{2}. Cell debris were removed by centrifugation (20,000 × *g* for 15 min at 4 °C), and cell extracts were used to measure PPC (Maeba and Sanwal, 1969). One unit of enzyme activity is the quantity of enzyme that converts 1 μmol of PEP to pyruvate per min. Total protein in the cell extracts

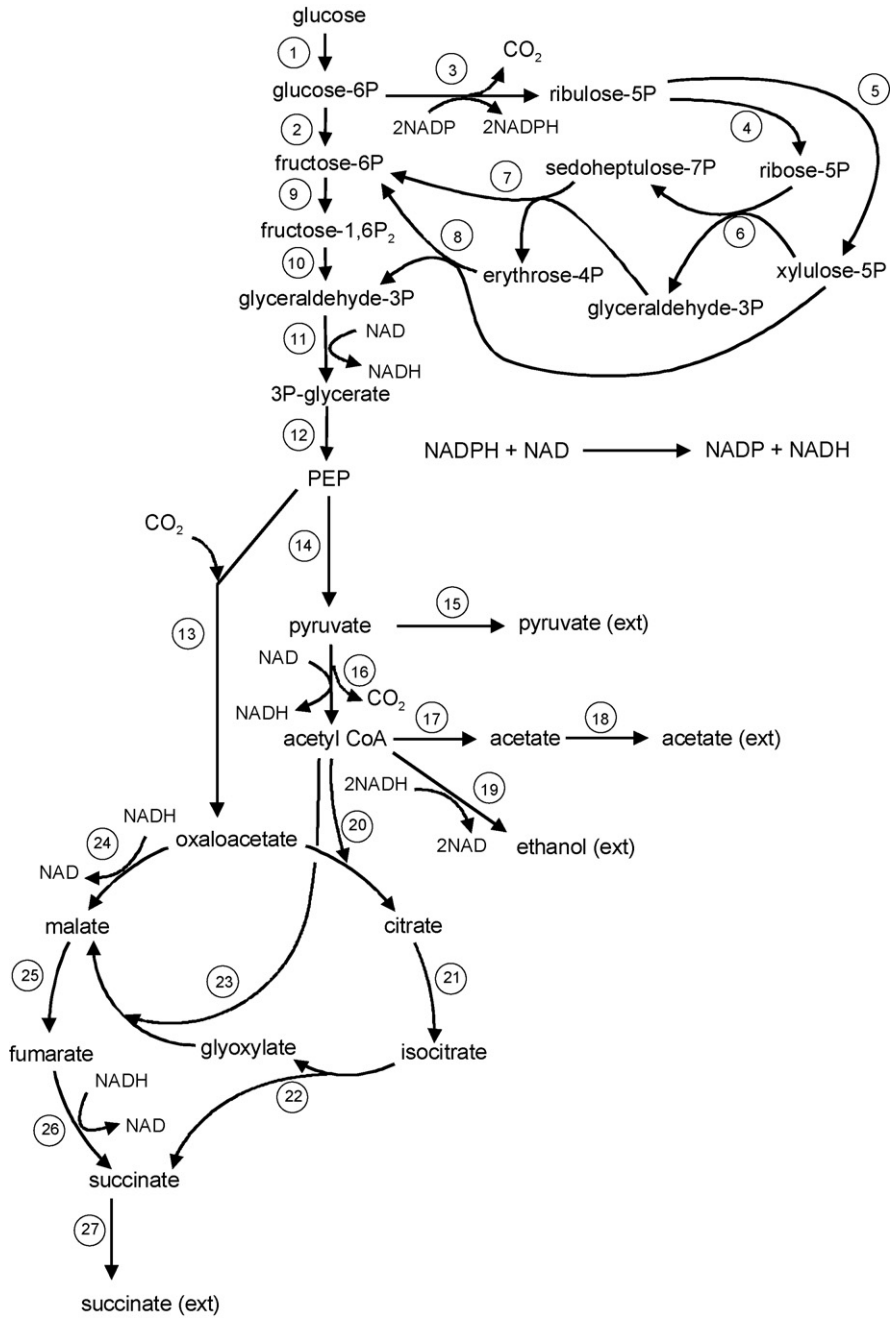

Fig. 2. Biochemical pathways for the synthesis of succinate from glucose in *E. coli*. Not all enzymatic steps or intermediates are shown. Key enzymes in the pathways are as follows: 1, glucokinase; 2, phosphoglucoisomerase; 3, 6-phosphogluconate dehydrogenase; 4, ribose-5P isomerase; 5, ribulose-5P 3-epimerase; 6, transketolase; 7, transaldolase; 8, transketolase; 9, phosphofructokinase; 10, fructose biphosphate aldolase; 11, glyceraldehyde 3-phosphate dehydrogenase and phosphoglycerate kinase; 12, phosphoglycerate mutase and enolase; 13, PEP carboxylase; 14, pyruvate kinase; 16, pyruvate dehydrogenase complex; 17, phosphoacetyltransferase and acetate kinase; 19, acetaldehyde dehydrogenase and alcohol dehydrogenase; 20, citrate synthase; 21, aconitase; 22, isocitrate lyase; 23, malate synthase; 24, malate dehydrogenase; 25, fumarase; and 26, fumarate reductase.

was determined with bovine serum albumin as the standard (Lowry et al., 1951).

3. Results

3.1. Effect of CO_2 concentration on succinate production

E. coli AFP111 accumulates significant amounts of succinate during an anaerobic non-growth phase after growing to a high cell density under aerobic conditions at a pH of 7.0. Succinate is formed through two pathways: the reductive arm of the tricarboxylic acid cycle via the anaplerotic enzyme PPC; and the glyoxylate shunt (Vemuri et al., 2002b). Since CO_2 is incorporated into the carbon backbone as a result of the carboxylation of PEP by PPC, we hypothesized that different CO_2 concentrations in the gas phase would impact the metabolic fluxes and ultimately change the yield and rate of succinate generated. We therefore conducted several fermentations using a constant agitation rate and total gas flowrate but with different levels of CO_2 in the gas phase during the anaerobic phase. Fig. 3 shows a typical dual-phase process with 50% CO_2 gas phase composition in the second anaerobic phase. Several products were generated: about 40 g/L succinate after 20 h with a yield

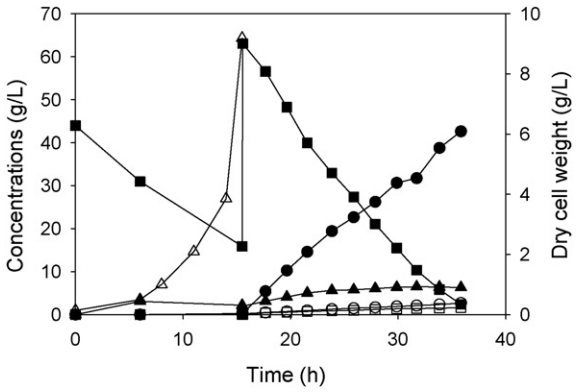

Fig. 3. Production of succinate (●), pyruvate (▲), ethanol (□), acetate (○) and dry cell weight (△) from glucose (■) in the dual-phase fermentation of *E. coli* AFP111. The switch from aerobic conditions to the anaerobic phase occurred at approximately 16 h, when a concentrated glucose solution was added to the bioreactor.

Table 1
Product yields of *E. coli* AFP111 during succinate production at different CO_2 concentrations in the gas phase.

CO_2 (%)	Y_S	Y_P	Y_A	Y_E
0	0.04 ± 0.02	ND	0.02 ± 0.01	ND
3	0.52 ± 0.03	0.19 ± 0.03	0.03 ± 0.01	0.02 ± 0.01
10	0.61 ± 0.04	0.16 ± 0.02	0.04 ± 0.01	0.03 ± 0.00
50	0.72 ± 0.08	0.10 ± 0.08	0.04 ± 0.02	0.03 ± 0.00
100	0.66 ± 0.03	0.12 ± 0.03	0.04 ± 0.00	0.03 ± 0.00

Observed values are shown as mean ± standard deviation from three analyses.
Y_S, Y_P, Y_A, and Y_E are yields of succinate, pyruvate, acetate and ethanol, respectively.
ND, non-detectable.

(Y_S) of 0.75 ± 0.08 g/g (mean ± standard deviation) at a specific rate (q_S) of 224.5 ± 27.2 mg/g h, while the by-products pyruvate, acetate, and ethanol had final concentrations of 2–6 g/L. The concentration of CO_2 in the gas phase did affect succinate formation (Table 1). In the absence of CO_2, almost no products accumulated, not surprising since CO_2 is required by *E. coli* AFP111 for the succinate pathway, and this organism has few other options to reoxide NAD(P)H. Between 3% and 50% CO_2, both q_S and Y_S increased with CO_2 concentration, but this trend did not extend beyond 50% CO_2 (Fig. 4). The yield of pyruvate (Y_P) decreased slightly with increasing CO_2 concentration up to 50% (Table 1). The yield for other by-products did not change significantly with CO_2 concentration (Table 1). The activity of PPC was measured to be 0.23 U/mg protein (and this value showed no trend with CO_2 concentration, presumably because this enzyme was expressed during the aerobic growth phase).

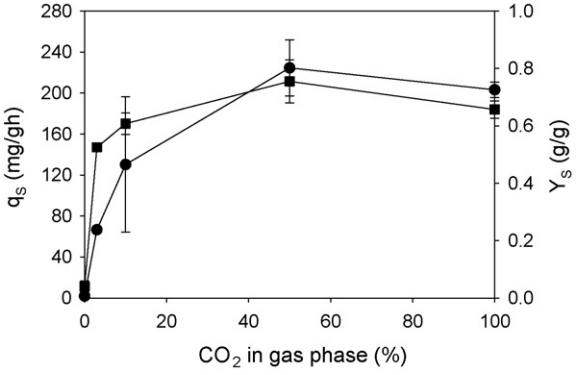

Fig. 4. Effect of gas phase CO_2 composition on succinate production: specific rate of succinate production, q_S (●) and mass yield Y_S (■). The anaerobic portion of the process operated at a pH of 6.40.

Table 2
Comparison of the mass distributions of succinate observed by mass spectrometry and those calculated by the error-minimized metabolic model. The enrichment ratio (S2/S1) was observed from NMR results. The redox ratio R/O was calculated using the metabolic model.

CO_2 (%)	φ_{PPP}	φ_{PPC}		M+0 (%)	M+1 (%)	M+2 (%)	M+3 (%)	(S2/S1)[a]	NAD(P)H generated (mmol/g h)	NAD(P)H consumed (mmol/g h)	R/O	Net ATP formed (mmol/g h)
3	0.04	0.53	Observed	0.594 ± 0.006	0.379 ± 0.003	0.023 ± 0.005	0.004 ± 0.002	17.03				
			Calculated	0.591	0.379	0.027	0.003	18.53	0.572	0.517	1.11	0.251
10	0.08	0.61	Observed	0.547 ± 0.005	0.417 ± 0.004	0.033 ± 0.003	0.003 ± 0.001	18.76				
			Calculated	0.549	0.418	0.030	0.004	20.64	3.294	3.274	1.01	1.173
50	0.17	0.63	Observed	0.586 ± 0.005	0.377 ± 0.011	0.031 ± 0.009	0.005 ± 0.005	17.53				
			Calculated	0.589	0.389	0.02	0.002	18.79	3.893	3.784	1.03	1.261

Observed values are shown as mean ± standard deviation from three analyses.
[a] The standard deviation for NMR measurements was 4–15%

3.2. Effect of CO_2 concentration on metabolic fluxes

In order to determine whether CO_2 affects the flux distribution, we conducted a series of fermentations in which 1-^{13}C-labeled glucose was added to the bioreactor during the succinate production phase. The known fluxes (glucose consumption and end-product formation rates) were calculated early during anaerobic conditions when the succinate concentration was less than 4 g/L. With these known fluxes and LC–MS results we then calculated the (error-minimized) flux distribution as described in Section 2. Table 2 compares the observed mass distribution of succinate and the calculated mass distribution. We further validated the metabolic model by comparing the enrichment ratio S2/S1 observed by NMR with the ratio calculated from the error-minimized metabolic model. The differences between the observed S2/S1 and the calculated values were less than 10% (Table 2), generally less than the error associated with the measurement. In addition, we calculated the R/O ratio based on the error-minimized model, and the values of this parameter for each CO_2 concentration were close to 1 (Table 2), supporting the balance for the oxidation and reduction of redox equivalents.

The metabolic fluxes calculated from the model indicate that CO_2 impacted the rates of substrate consumption and product formation. An increase in gas phase CO_2 concentration from 3% to 50% increased both the glucose consumption rate and succinate production rate six-fold (Fig. 5). Also, the fraction of flux into the pentose phosphate pathway (φ_{PPP}) increased from 0.04 at 3% CO_2 to 0.17 at 50% CO_2 (Table 2 and Fig. 5). The fraction of flux through the carboxylation at the PEP node (φ_{PPC}) increased from 0.53 to 0.63 between 3% CO_2 and 50% CO_2 (Table 2 and Fig. 5). Slightly more

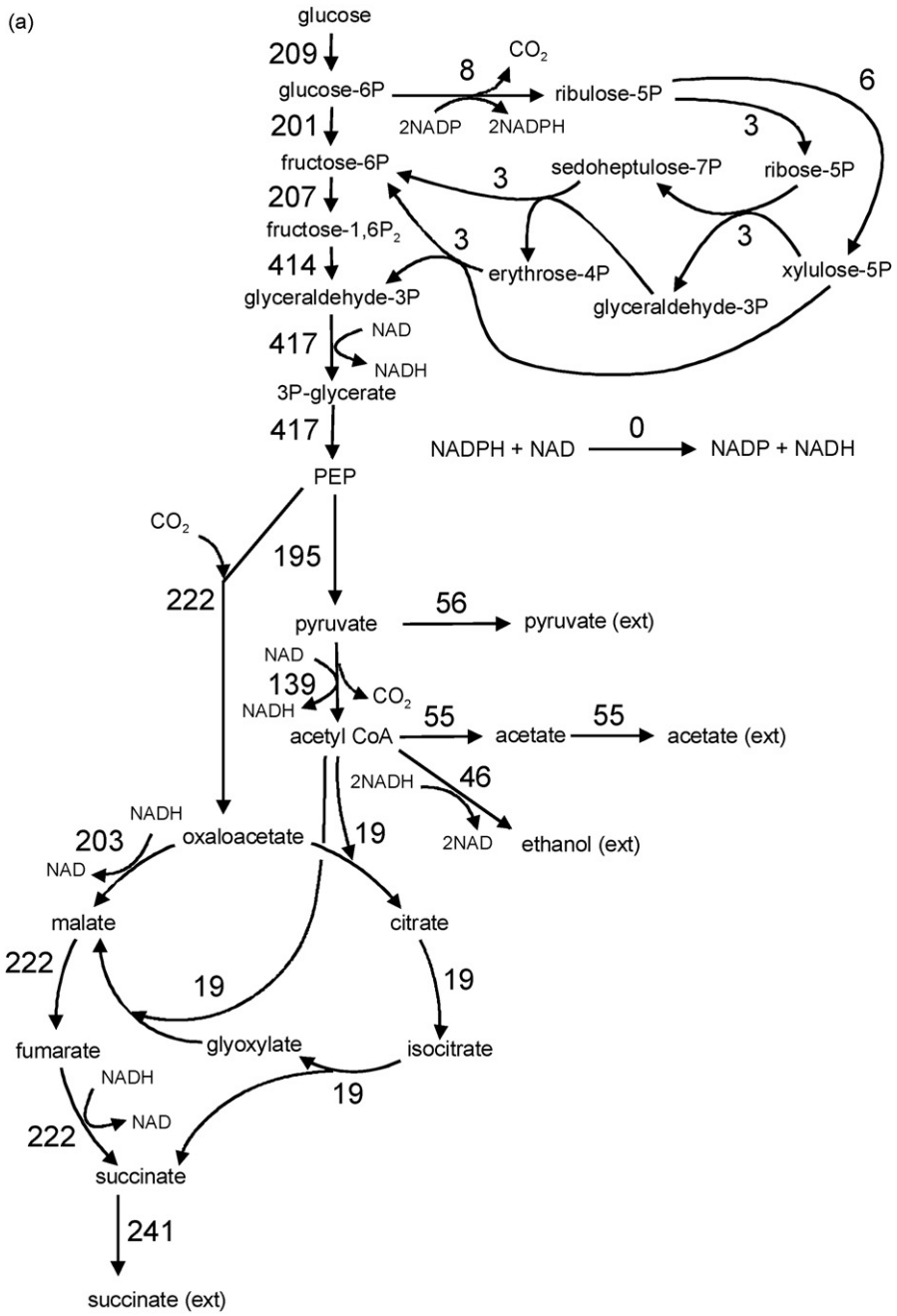

Fig. 5. Fluxes through biochemical pathways at three CO_2 concentrations: (a) 3% CO_2; (b) 10% CO_2 and (c) 50% CO_2. The units of the flux are μmol/g h.

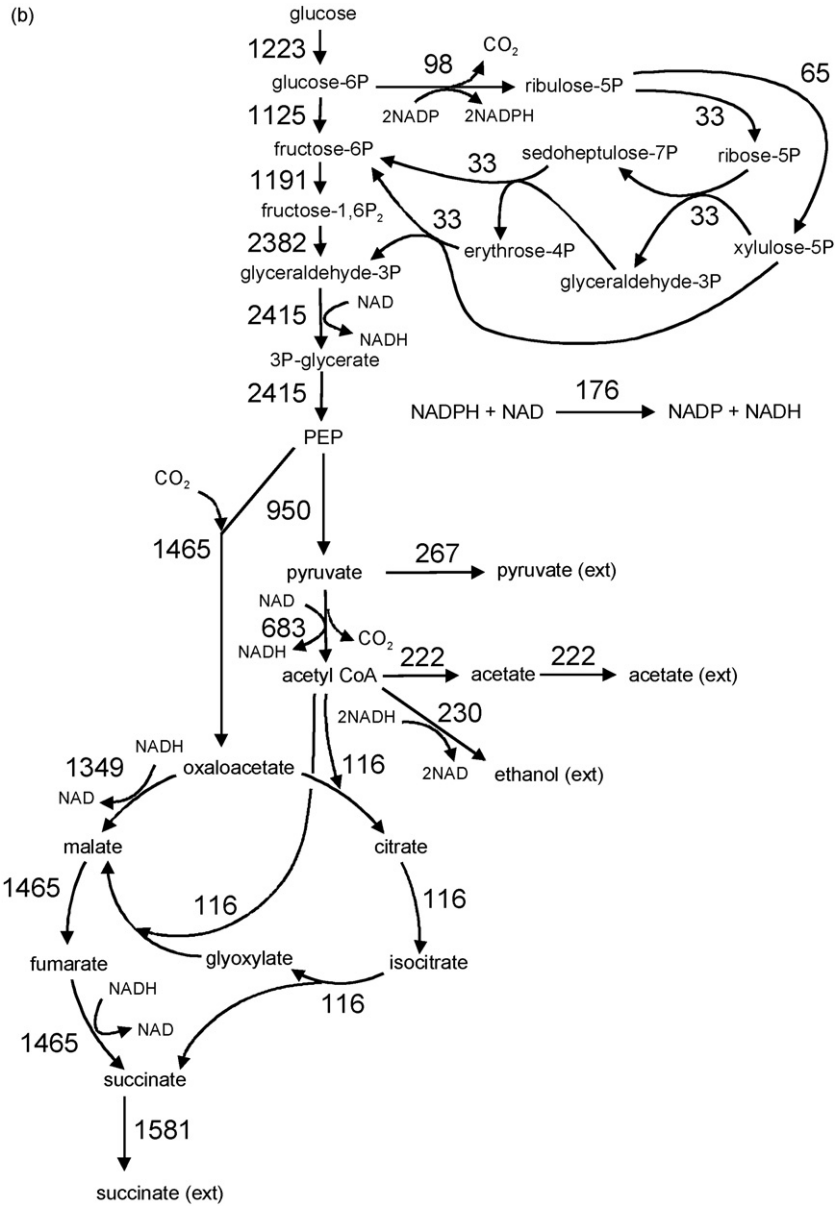

Fig. 5. (*Continued*)

succinate was formed via the reductive arm of the TCA cycle at 50% CO_2 than at 3% CO_2 (88% versus 85%). Pyruvate formation decreased slightly due to reduced glycolysis and reduced flux through pyruvate dehydrogenase at the PEP node (Fig. 5), consistent with the previous experiments (Table 1). Some pathways generate CO_2 while one pathway consumes CO_2 during succinate formation. Specifically, CO_2 was generated via 6-phosphogluconate dehydrogenase and pyruvate dehydrogenase (or pyruvate oxidase) but consumed via PPC (Fig. 2). A CO_2 concentration of 3% resulted in a net CO_2 consumption rate of 0.08 mmol/g h (3.5 mg/g h) with an overall stoichiometric coefficient for CO_2 (i.e., the molar ratio of net CO_2 consumption to glucose consumption) of 0.36. In comparison, a CO_2 concentration of 50% led to an overall stoichiometric CO_2 coefficient of 0.53 and a net consumption rate of 0.73 mmol/g h (32 mg/g h), corresponding to a volumetric CO_2 consumption rate of 288 mg/L h.

3.3. Effect of agitation rate

Mass transfer could potentially be a limiting factor when the CO_2 concentration decreases. We therefore also studied 10% CO_2 but used higher agitation rates (400 rpm and 1000 rpm) to increase the CO_2 mass transfer rate. Higher agitation rates did not alter observed values of q_S and Y_S (Fig. 6), providing strong evidence that mass transfer of gaseous CO_2 was not limiting at this CO_2 concentration. The generation of all other by-products also remained unchanged (data not shown).

4. Discussion

NMR, LC–MS and HPLC analyses using ^{13}C-labeled substrates were successfully combined to calculate metabolic fluxes during succinate production at different levels of CO_2. The LC–MS provides the numbers of labeled carbon atoms but not the labeled position, while NMR results provide information about position. For example, the MS cannot distinguish between [1-^{13}C] succinate and [2-^{13}C] succinate while NMR generates a different pattern with these two specific isotopomers. The small difference between observed and predicted enrichment ratio S2/S1 (less than 10%), as well as a calculated R/O ratio near 1 provide strong evidence for the appropriateness of our metabolic model describing succinate

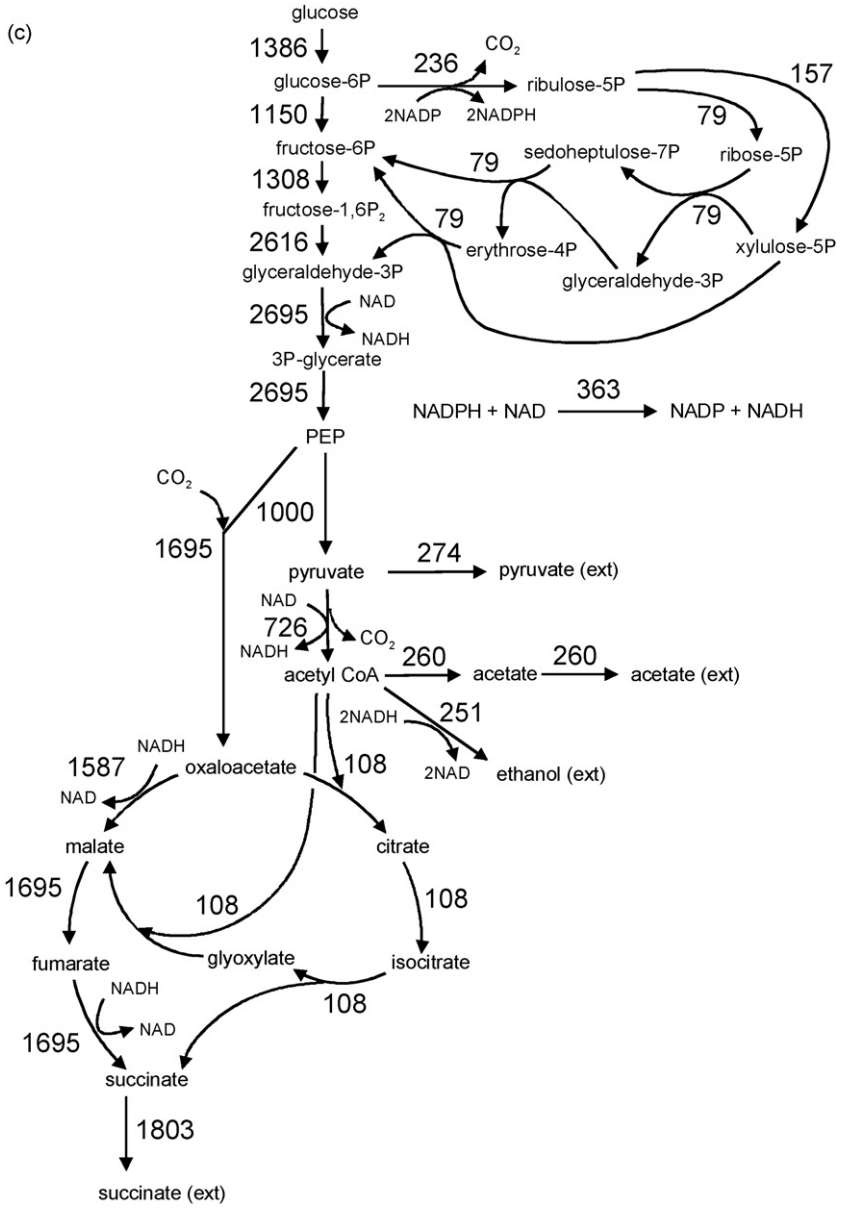

Fig. 5. (*Continued*).

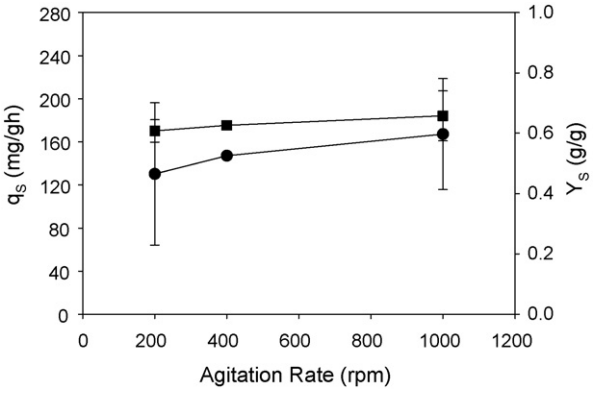

Fig. 6. Effect of agitation on succinate production: specific rate of production, q_S (●) and mass yield Y_S (■). The anaerobic portion of the process operated at a pH of 6.4 and 10% CO_2 in the gas phase.

production during an anaerobic non-growth phase. Although the model is a simplification of metabolism, and error may occur from some anabolic reactions, these reactions are likely minimal because the cells are not growing significantly during the anaerobic phase. Another source of error may be alternate catabolic reactions.

Succinate is principally formed through two pathways: the reductive arm of the TCA cycle and the glyoxylate shunt (Clark, 1989; Vemuri et al., 2002b). Through the reductive arm of the TCA cycle CO_2 is incorporated into the final product succinate via the enzyme PPC. This gas is therefore necessary for succinate production, and CO_2 availability impacts substrate utilization and product accumulation rates. Not surprisingly, in our study increasing CO_2 concentrations in the gas phase increased the succinate production, and ^{13}C-flux analysis demonstrated that more carbon partitioned at the PEP node into the reductive arm of the TCA cycle. As a result more CO_2 was incorporated into the carbon backbone, and the overall stoichiometric coefficient increased from 0.36 at 3% CO_2 to 0.53 at 50% CO_2. Since succinate formation through the reductive arm of the TCA cycle is not redox balanced with glucose (Vemuri et

al., 2002a), a consequence of higher flux through PPC to succinate is a greater demand on reduced cofactors. The cells unexpectedly responded to an increased concentration of CO_2 in the gas phase by increasing the relative flux through the pentose phosphate pathway (Table 2), which paradoxically itself is a CO_2-generating pathway. Since the conversion of 1 mol glucose to PEP via glycolysis generates 2 mol of NADH while the conversion of 1 mol glucose to PEP via the pentose phosphate pathway generates 3.67 mol of NAD(P)H, increased pentose phosphate pathway flux is a means to meet the elevated demand for reduced cofactors. Our studies did not establish the specific mechanism by which the pentose phosphate pathway is upregulated.

NADPH is primarily generated in the pentose phosphate pathway, but NADH is consumed during succinate formation through the reductive arm of the TCA cycle. Therefore, insufficient capacity to reoxidize NADPH could limit succinate formation. However, NADPH and NADH are interconvertible by transhydrogenases (Sauer et al., 2004), and previous results suggest *E. coli* has sufficient capacity in succinate production (Fuhrer and Sauer, 2009). In particular, during aerobic growth *E. coli* generates about 30 U/g transhydrogenase, which in our study would correspond to a potential flux of about 0.8 mmol/g h. For each of the three conditions examined (Fig. 5a–c) the calculated transhydrogenase flux was lower than 0.8 mmol/g h.

Elevated CO_2 in the gas phase promotes additional CO_2 generation by the pentose phosphate pathway, and this additional CO_2 would contain the label from 1-^{13}C-glucose as a result of the action of phosphogluconate dehydrogenase. However, we did not observe significant incorporation of labeled CO_2 into succinate via PPC probably because the moderately high gas flowrate used in our experiments diluted the much lower quantity of labeled CO_2 that would be generated in the pentose phosphate pathway.

Our results suggest that CO_2 limited succinate formation only at low CO_2 concentrations (i.e., around 10% CO_2 in gas phase). From the metabolic flux analysis, about 90% of the succinate generated involved CO_2 incorporation by PPC. Thus, the maximum CO_2 consumption rate *per cell* ($J^{MAX}_{CO_2}$) is 90% of the specific succinate production rate during the anaerobic phase:

$$J^{MAX}_{CO_2} = \frac{0.9 q_s}{M/m_E}$$

where M is molar mass of succinate (116 g/mol), and m_E is the average dry weight of an *E. coli* cell, 2.9×10^{-13} g (Neidhardt et al., 1996). Based on our experimental results at 50% CO_2, $J^{MAX}_{CO_2}$ is 1.4×10^{-16} mmol/s.

How does CO_2 limit succinate formation? Through the reductive branch of TCA cycle, the utilization of gaseous CO_2 and its ultimate conversion to succinate can be described by four separate processes (Fig. 7): (1) the transport of CO_2 from the gas phase to the bulk liquid phase, (2) the transport of CO_2 from the bulk liquid phase across the cell membrane into the cytoplasm, (3) the intracellular conversion of dissolved CO_2 into bicarbonate, (4) the incorporation of bicarbonate to form oxaloacetate due to the enzyme PPC.The flux of CO_2 transport from the gas (bubble) sparged into the fermenter to the liquid phase ($J^1_{CO_2}$), is proportional to the mass transfer coefficient:

$$J^1_{CO_2} = \frac{1}{(X/m_E)} \frac{d[CO_2]_{ex}}{dt} = \frac{k_L a_{(CO_2)}([CO^*_2] - [CO^l_2]_{ex})}{X/m_E} = \frac{k_L a_{(CO_2)} \Delta[CO_2]}{X/m_E} \quad (1)$$

where k_La is the volumetric CO_2 mass transfer coefficient (s^{-1}), $[CO^*_2]$ is the molar CO_2 concentration in equilibrium with the gas phase, $[CO^l_2]_{ex}$ is the molar (extracellular) liquid phase CO_2 concentration, and X is dry cell density (g/L). We measured the oxygen mass transfer coefficient in our system at identical conditions (e.g., 200 rpm and 1.2 L) and using a correlation (Royce and Thornhill, 1991), estimate the value of $k_La_{(CO_2)}$ to be 0.0081 s^{-1}. Using a value for X of 8.4 g/L, at steady-state (with no accumulation of CO_2 or HCO_3^-)

$$J^1_{CO_2} = \frac{k_L a_{(CO_2)} \Delta[CO_2]}{X/m_E} = 1.4 \times 10^{-16} \text{ mmol/s} \quad (2)$$

The driving force $\Delta[CO_2]$ is at most 0.5 mmol/L. If the value of $[CO^*_2]$ is large, then the value of $[CO^l_2]_{ex}$ is relatively close to $[CO^*_2]$. For example, if the partial pressure of CO_2 is 0.10 atm, then $[CO^*_2]$ is 3.8 mM (Carroll et al., 1991) and $[CO^l_2]_{ex}$ is 3.3 mM, which is only 13% less than the equilibrium concentration. At a CO_2 partial pressure of 0.50 atm, $[CO^l_2]_{ex}$ would be about 18.5 mM, almost indistinguishable from the equilibrium concentration $[CO^*_2]$ and thus no mass transfer limitation would occur. From this analysis we conclude that at gas phase concentrations of CO_2 greater than 2–3%, mass transfer would not limit CO_2 utilization under these conditions, a conclusion consistent with our results using higher agitation rates (Fig. 6).

The second process which could limit the succinate formation process is the diffusion of dissolved CO_2 through the cell membrane. Permeation of HCO_3^- through the lipid membrane is insignificant (Gutknecht et al., 1977). For rod-shaped cells (Berg, 1983; Neidhardt et al., 1996), the CO_2 diffusion rate through one cell ($J^2_{CO_2}$) is given by:

$$J^2_{CO_2} = PA_E([CO^l_2]_{ex} - [CO^l_2]_{in}) \quad (3)$$

The permeability coefficient P is 3.5×10^{-3} m/s (Gutknecht et al., 1977), and A_E is the surface area of an *E. coli* cell is 6×10^{-12} m^2 (Neidhardt et al., 1996). Setting $J^2_{CO_2}$ equal to the maximum flux, $[CO^l_2]_{in}$ is essentially identical to $[CO^l_2]_{ex}$ even for low values of $[CO^l_2]_{ex}$ demonstrating diffusion of CO_2 across the cell membrane does not limit CO_2 utilization.

The third process is the intracellular chemical hydration of CO_2 to HCO_3^-, described by the following equilibrium:

$$CO_2 + H_2O \underset{k_{-1}}{\overset{k_1}{\rightleftarrows}} HCO_3^- + H^+$$

where k_1 is 0.029 s^{-1}, and k_{-1} is 2.0×10^4 L/mol s (Pocker and Bjorkquist, 1977). Accordingly, the CO_2 conversion rate is

$$J^3_{CO_2} = (k_1[CO^l_2]_{in} - k_{-1}[HCO_3^-][H^+])V_E \quad (4)$$

where V_E is the cytoplasm volume of an *E. coli* cell, about 1.0×10^{-15} L (Neidhardt et al., 1996). The maximum flux occurs when there is no bicarbonate ion to act as a reactant for the reverse

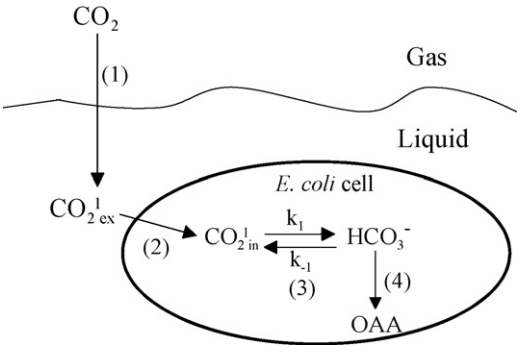

Fig. 7. Explicit model of CO_2 transport and utilization by *E. coli* cell. OAA is oxaloacetate.

reaction:

$$J^3_{CO_2}(\max) = k_1[CO^l_2]_{in}V_E \quad (5)$$

For the example of $[CO^l_2]_{in}$ = 3.3 mM, as calculated above with 10% CO_2 in the gas phase, the maximum flux $J^3_{CO_2}(\max)$ is about 9.6×10^{-17} mmol/s, more than 30% less than the value for $J^{MAX}_{CO_2}$ of 1.4×10^{-16} mmol/s. If the gas phase concentration is 50%, then $J^3_{CO_2}(\max)$ is 5.3×10^{-16} mmol/s, and this third process would be less likely to be limiting. This analysis indicates that the third step may be rate limiting at a low concentration of CO_2 (i.e., 10%), preventing the succinate production pathway to operate at its maximum rate. This analysis does not consider the enzymatic conversion of dissolved CO_2 to bicarbonate mediated by the enzyme carbonic anhydrase.

The fourth process is the utilization of HCO_3^- by the enzyme PPC, and its rate is

$$J^4_{CO_2} = \frac{V_{(PPC)}[HCO_3^-]}{(K_{M(PPC)} + [HCO_3^-])} \quad (6)$$

where $K_{M(PPC)}$ is the Michaelis–Menten constant with a value of 0.1 mM for the *E. coli* enzyme (Kai et al., 1999), and $V_{(PPC)}$ is the maximum rate of HCO_3^- utilization by PPC [in mmol/s]. In order to use Eq. (6) to estimate the maximum value for $J^4_{CO_2}$, a value is needed for $[HCO_3^-]$. At the pseudo-steady-state of the process, the rate change of $[HCO_3^-]$ equals zero:

$$V_E\frac{d[HCO_3^-]}{dt} = (k_1[CO^l_2]_{in} - k_{-1}[HCO_3^-][H^+])V_E - \frac{V_{(PPC)}[HCO_3^-]}{(K_{M(PPC)} + [HCO_3^-])} = 0 \quad (7)$$

Using the value of 0.23 U/mg (the value measured at 50% CO_2) and the cell concentration of 3×10^{13} cells/L (data not shown), we find the maximum enzyme activity is 2.8×10^{-11} U/cell or 4.6×10^{-16} mmol product formed/s. At 10% CO_2 with $[CO^l_2]_{in}$ = 3.3 mM and an intracellular pH of 7.0 (Olsen et al., 2002), the calculated $[HCO_3^-]$ is 0.026 mM. This concentration is only one-fourth the value of K_M, so that the enzymatic reaction occurs only at 20% of the maximum $V_{(PPC)}$, resulting in a value for $J^4_{CO_2}$ of 9.5×10^{-17} mmol/s. At 50% CO_2, the bicarbonate concentration far exceeds the value of K_M. Indeed, according to Eq. (7) the intracellular bicarbonate concentration is very sensitive to gas phase CO_2 concentration (Fig. 8), demonstrating that the enzyme reaction is potentially limiting at 10% CO_2 (because of low $[HCO_3^-]$), whereas at higher CO_2 concentrations, the intrinsic activity of the enzyme could limit the overall process. At approximately $[CO^l_2]_{in}$ equal to 15 mM, the concentration of HCO_3^- quickly becomes much higher than $K_{M(PPC)}$ (Fig. 8). This concentration corresponds with a CO_2 concentration of about 30–40% in the gas phase to meet the requirement for the succinate production pathway running at its maximum. Not included in this analysis are the various unknown concentrations of affectors of PPC, such as aspartate and citrate (Gold and Smith, 1974), which would further limit activity *in vivo*, particularly at high bicarbonate concentrations. Also, this analysis does not consider possible indirect effects, such as CO_2 affecting another enzyme in one of the succinate pathways, or for example, the observation that succinate inhibits the activity of PPC (Gold and Smith, 1974).

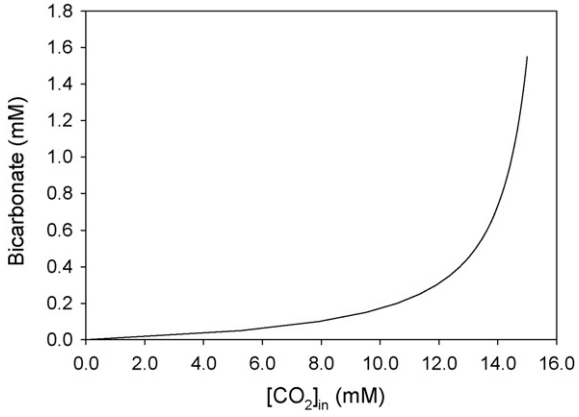

Fig. 8. Relationship between $[CO^l_2]_{in}$ and $[HCO_3^-]$ in the succinate production system using Eq. (7).

The results of the analysis of the four processes involved in the incorporation of CO_2 into succinate indicate that enzymatic processes are rate limiting over most of the range of gas phase CO_2 concentrations. However, the reason for the limitation may change. At very high CO_2 concentrations, the activity of the enzyme ($V_{(PPC)}$) likely limits CO_2 utilization, whereas at intermediate CO_2 concentrations (10–30%), the HCO_3^- concentration can limit CO_2 utilization. Only at very low CO_2 concentrations (less than 3%) would mass transfer limit CO_2 utilization.

This analysis also suggests strategies to improve CO_2 utilization. For example, at intermediate CO_2 concentrations, overexpression of the carbonic anhydrase enzyme which catalyzes the hydration of CO_2 to HCO_3^- might be effective. If pure CO_2 were used, further improvement in succinate production should result from increased enzyme expression, as has been previously observed with the pyruvate carboxylase enzyme (Vemuri et al., 2002b). Of course, elevated enzyme expression can have limited benefit because of other affectors. Mass transfer should be considered as a potential benefit only for very low CO_2 concentrations.

This study demonstrates that CO_2 is essential to PEP carboxylation, which leads to the accumulation of succinate through the reductive branch of the TCA cycle by *E. coli* AFP111. Metabolic flux analysis with ^{13}C-labeled glucose allowed an understanding of the carbon flux partitioning of *E. coli* AFP111 in response to varied CO_2 concentrations, including the surprising observation that CO_2 affected the fraction of flux into the pentose phosphate pathway.

Acknowledgments

We thank U.S. Department of Energy (DE-FG26-04NT42126) and Georgia Experiment Stations for financial support. We acknowledge Drs. D.R. Phillips, T.M. Andacht, and G.P. Wylie for LC–MS and NMR analyses. We thank S.A. Lee, R. Altman, and Y. Ma for technical assistance, and Dr. J.L. Urbauer for helpful discussions.

Appendix A. Metabolic reactions for succinate production

v_1:	Glucose + ATP ⇆ glucose 6-phosphate + ADP
v_2:	Glucose 6-phosphate ⇆ fructose 6-phosphate
v_3:	Glucose 6-phosphate + 2NADP$^+$ + H_2O ⇆ ribulose 5-phosphate + CO_2 + 2NADPH + 2H^+
v_4:	Ribulose 5-phosphate ⇆ ribose-5-phosphate
v_5:	Ribulose 5-phosphate ⇆ xylulose 5-phosphate
v_6:	Ribose 5-phosphate + xylulose 5-phosphate ⇆ glyceraldehyde 3-phosphate + sedoheptulose 7-phosphate
v_7:	Glyceraldehyde 3-phosphate + sedoheptulose-7-phosphate ⇆ fructose 6-phosphate + erythrose 4-phosphate
v_8:	Xylulose 5-phosphate + erythrose 4-phosphate ⇆ fructose 6-phosphate + glyceraldehydes 3-phosphate
v_9:	Fructose 6-phosphate + ATP ⇆ fructose 1,6-bisphosphate + ADP
v_{10}:	Fructose 1,6-bisphosphate ⇆ dihydroxyacetone phosphate + glyceraldehyde 3-phosphate

v_{11}:	Glyceraldehyde 3-phosphate + NAD^+ + ADP + Pi ⇆ 3-phosphoglycerate + NADH + H^+ + ATP
v_{12}:	3-Phosphoglycerate ⇆ PEP + H_2O
v_{13}:	PEP + CO_2 + H_2O ⇆ oxaloacetate + Pi
v_{14}:	Phosphoenolpyruvate + ADP ⇆ pyruvate + ATP
v_{15}:	Pyruvate (intracellular) ⇆ pyruvate (extracellular)
v_{16}:	Pyruvate + NAD^+ + CoA ⇆ acetyl-CoA + CO_2 + NADH + H^+
v_{17}:	Acetyl-CoA + ADP + Pi ⇆ acetate + CoA + ATP
v_{18}:	Acetate (intracellular) ⇆ acetate (extracellular)
v_{19}:	Acetyl-CoA + 2NADH + $2H^+$ ⇆ ethanol + $2NAD^+$
v_{20}:	Oxaloacetate + acetyl-CoA + H_2O ⇆ citrate + CoA
v_{21}:	Citrate ⇆ isocitrate
v_{22}:	Isocitrate ⇆ glyoxylate + succinate
v_{23}:	Glyoxylate + acetyl-CoA + H_2O ⇆ malate + CoA
v_{24}:	Oxaloacetate + NADH + H^+ ⇆ malate + NAD^+
v_{25}:	Malate ⇆ fumarate + H_2O
v_{26}:	Fumarate + NADH + H^+ ⇆ succinate + NAD^+
v_{27}:	Succinate (intracellular) ⇆ succinate (extracellular)

References

Atom, H., 2002. Microbial enzymes involved in carbon dioxide fixation. J. Biosci. Bioeng. 94, 497–505.

Berg, H.C., 1983. Diffusion: macroscopic theory. In: Random Walks in Biology. Princeton University Press, Princeton, New Jersey.

Brown, L., 1996. Uptake of carbon dioxide from flue gas by microalgae. Energy Convers. Manage. 37, 1363–1367.

Carroll, J., Slupsky, J., Mather, A., 1991. The solubility of carbon dioxide in water at low pressure. J. Phys. Chem. Ref. Data 20, 1201–1209.

Chatterjee, R., Millard, C.S., Champion, K., Clark, D.P., Donnelly, M.I., 2001. Mutation of the *ptsG* gene results in increased production of succinate in fermentation of glucose by *Escherichia coli*. Appl. Environ. Microbiol. 67, 148–154.

Clark, D.P., 1989. The fermentation pathways of *Escherichia coli*. FEMS Microbiol. Rev. 63, 223–234.

Donnelly, M.I., Millard, C.S., Clark, D.P., Chen, M.J., Rathke, J.W., 1998. A novel fermentation pathway in an *Escherichia coli* mutant producing succinic acid, acetic acid, and ethanol. Appl. Biochem. Biotechnol. 70–72, 187–198.

Eiteman, M.A., Chastain, M.J., 1997. Optimization of the ion-exchange analysis of organic acids from fermentation. Anal. Chim. Acta 338, 69–75.

Fleurence, J., 1999. Seaweed proteins: biochemical, nutritional aspects and potential uses. Trends Food. Sci. Technol. 10, 25–28.

Fuhrer, T., Sauer, U., 2009. Different biochemical mechanisms ensure network-wide balancing of reducing equivalents in microbial metabolism. J. Biotechnol. 191, 2112–2121.

Gold, E.W., Smith, T.E., 1974. *Escherichia coli* phosphoenolpyruvate carboxylase: effect of allosteric inhibitors on the kinetic parameters and sedimentation behavior. Arch. Biochem. Biophys. 164, 447–455.

Gutknecht, J., Bisson, M., Tosteson, F., 1977. Diffusion of carbon dioxide through lipid bilayer membranes: effects of carbonic anhydrase, bicarbonate, and unstirred layers. J. Gen. Physiol. 69, 779–794.

Kai, Y., Matsumura, H., Inoue, T., Terada, K., Nagara, Y., Yoshinaga, T., Kihara, A., Tsumura, K., Izui, K., 1999. Three-dimensional structure of phosphoenolpyruvate carboxylase: a proposed mechanism for allosteric inhibition. Proc. Natl. Acad. Sci. 96, 823–828.

Lowry, O., Rosebrough, N., Farr, A., Randall, R., 1951. Protein measurement with Folin phenol reagent. J. Biol. Chem. 193, 265–275.

Maeba, P., Sanwal, B., 1969. Phosphoenolpyruvate carboxylase of *Salmonella.* Some chemical and allosteric properties. J. Biol. Chem. 244, 2549–2557.

Matsumura, H., Xie, Y., Shirakata, S., Inoue, T., Yoshinaga, T., Ueno, Y., Izui, K., Kai, Y., 2002. Crystal structures of C4 form maize and quaternary complex of *E. coli* phosphoenolpyruvate carboxylases. Structure (Camb) 10, 1721–1730.

Matte, A., Tari, L.W., Goldie, H., Delbaere, L.T.J., 1997. Structure and mechanism of phosphoenolpyruvate carboxykinase. J. Biol. Chem. 272, 8105–8108.

McKinlay, J.B., Shachar-Hill, Y., Zeikus, J.G., Vieille, C., 2007. Determining *Actinobacillus succinogenes* metabolic pathways and fluxes by NMR and GC–MS analyses of 13C-labeled metabolic products isotopomers. Metab. Eng. 9, 177–192.

Modak, H.V., Kelly, D.J., 1995. Acetyl-CoA-dependent pyruvate carboxylase from the photosynthetic bacterium *Rhodobacter capsulatus*: rapid and efficient purification using dye-ligand affinity chromatography. Microbiology 141, 2619–2628.

Neidhardt, F.C., Curtiss III, R., Ingraham, J.L., Lin, E.C.C., Low Jr., K.B., Magasanik, B., Reznikoff, W.S., Riley, M., Schaechter, M., Umbarger, H.E. (Eds.), 1996. *Escherichia coli* and *Salmonella typhimurium*: cellular and molecular biology, 2nd ed. ASM Press, Washington, D.C..

Olsen, K., Budde, B., Siegumfeldt, H., Rechinger, K., Jakobsen, M., Ingmer, H., 2002. Noninvasive measurement of bacterial intracellular pH on a single-cell level with green fluorescent protein and fluorescence ratio imaging microscopy. Appl. Environ. Microbiol. 68, 4145–4147.

Otsuki, T., 2001. A study for the biological CO_2 fixation and utilization system. Sci. Total Environ. 277, 21–25.

Pocker, Y., Bjorkquist, D.W., 1977. Stopped-flow studies of carbon dioxide hydration and bicarbonate dehydration in H_2O and D_2O. Acid-base and metal ion catalysis. J. Am. Chem. Sot. 99, 6537–6543.

Royce, P.N.C., Thornhill, N.F., 1991. Estimation of dissolved carbon dioxide concentrations in aerobic fermentations. AIChE J. 37, 1680–1686.

Rosman, K.J.R., Taylor, P.D.P., 1998. Isotopic compositions of the elements. Pure Appl. Chem. 70, 217–230.

Sauer, U., Canonaco, F., Heri, S., Perrenoud, A., Fischer, E., 2004. The soluble and membrane-bound transhydrogenases *UdhA* and *PntAB* have divergent functions in NADPH metabolism of *Escherichia coli*. J. Biol. Chem. 279, 6613–6619.

Savinell, J.M., Palsson, B.O., 1992. Network analysis of intermediary metabolism using linear optimisation. I. Development of mathematical formalism. J. Theor. Biol. 154, 421–454.

Shively, J.M., van Keulen, G., Meijer, W.G., 1998. Something from almost nothing: carbon dioxide fixation in chemoautotrophs. Annu. Rev. Microbiol. 52, 191–230.

Schmidt, K., Carlsen, M., Nielsen, J., Villadsen, J., 1997. Modeling isotopomer distributions in biochemical networks using isotopomer mapping matrices. Biotechnol. Bioeng. 55, 831–840.

Spolaore, P., Joannis-Cassan, C., Duran, E., Isambert, A., 2006. Commercial applications of microalgae. J. Biosci. Bioeng. 101, 87–96.

Ugurbil, K., Brown, T.R., den Hollander, J.A., Glynn, P., Shulman, R.G., 1978. High-resolution 13C nuclear magnetic resonance studies of glucose metabolism in *Escherichia coli*. Proc. Natl. Acad. Sci. U.S.A. 75, 3742–3746.

Van Dien, S.J., Strovas, T., Lidstroml, M.E., 2003. Quantification of central metabolic fluxes in the facultative methylotroph *methylobacterium extorquens* AM1 using ^{13}C-label tracing and mass spectrometry. Biotechnol. Bioeng. 84, 45–55.

Vemuri, G.N., Eiteman, M.A., Altman, E., 2002a. Effects of growth mode and pyruvate carboxylase on succinic acid production by metabolically engineered strains of *Escherichia coli*. Appl. Environ. Microbiol. 68, 1715–1727.

Vemuri, G.N., Eiteman, M.A., Altman, E., 2002b. Succinate production in dual-phase *Escherichia coli* fermentations depends on the time of transition from aerobic to anaerobic conditions. J. Ind. Microbiol. Biotechnol. 28, 325–332.

Watanabe, Y., Hall, D.O., 1996. Photosynthetic CO_2 conversion technologies using a photobioreactor incorporating microalgae-energy and material balance. Energy Convers. Manage. 37, 1321–1326.

Zhang, K., Kurano, N., Miyachi, S., 2002. Optimized aeration by carbon dioxide gas for microalgal production and mass transfer characterization in a vertical flat-plate photobioreactor. Bioprocess Biosyst. Eng. 25, 97–101.